Structural Transformation of Au−Pd Bimetallic Nanoclusters on Thermal Heating and Cooling: A Dynamic Analysis

H. B. Liu,*,† U. Pal,*,‡ R. Perez,† and J. A. Ascencio†

Programa de Investigación en Ductos, Materiales y Corrosión, Instituto Mexicano del Petróleo, Eje Central Lázaro Cárdenas No. 152, Col. San Bartolo Atepehuacan, C.P.07730, México D.F., Mexico, and Instituto de Física, Universidad Autónoma de Puebla, Apdo. Postal J-48, Puebla, Pue. 72570, Mexico

Received: October 22, 2005; In Final Form: January 13, 2006

Classical molecular dynamics simulation is used for structural thermodynamic and dynamic analysis of Au−Pd bimetallic clusters. It is observed that the Pd-core/Au-shell structure is the most stable, and can be formed through annealing of other structures such as Au-core/Pd-shell, eutecticlike, or solid solution. Depending on the starting temperature and initial composition, three-layer icosahedral nanorod, face-centered cubic (fcc) nanorod, and fcc cluster can be obtained on slow cooling. The three-layer icosahedral nanorod structure is not as stable as the Pd-core/Au-shell decahedron; however it is more stable than the solid-solution decahedron structure up to 400 K. Our findings provide valuable insight into catalysis using Au−Pd and other similar bimetallic clusters.

I. Introduction

Bimetallic nanoclusters have received considerable attention recently[1] for their unique properties, which are very different from those of pure clusters of their constituents[2,3] and for a wide range of technological applications, ranging from catalysis to optics.[4,5] The properties of bimetallic nanoclusters vary not only with their size but also with their chemical compositions. Recent success in application of bimetallic nanoclusters has generated great interest on their design, synthesis, and characterization.[6−9] Among the bimetallic nanoclusters, Au−Pd is the most attractive catalyst for the hydrodesulfurization of thiophene,[10] direct synthesis of hydrogen peroxide from H_2 and O_2, etc.[11−13] Recently they have been developed for nanocontact applications.[14] Catalytic performance of Au−Pd bimetallic nanoclusters benefits to a great extent from their structural diversities, such as alloy cluster,[15−22] wire,[23] lithography,[24] and core/shell.[25−27] From the point of view of the phase diagram, Au−Pd is likely to form unlimited solid solutions at low temperatures.[28] The dilute-limit heat of solution of Au in Pd host is about −0.33 eV and of Pd in Au host is about −0.29 eV,[29] which are consistent with the formation of a variety of bimetallic structures. While the size, shape, composition, and atomic distribution of the nanoclusters are the key parameters for catalyst design, studies of structural dynamics and thermodynamic behavior are essential for their applications. In our previous work,[30] structural incoherency and thermodynamic stability of Au−Pd nanoclusters were studied systematically. In the present work, we report on thermal effects and dynamic analysis of structural transformation of Au−Pd nanoclusters through molecular dynamics (MD) simulation.

II. Research Methods

A simple analytical embedded-atom model (EAM) developed by Cai et al.[31] is used to describe the interatomic interaction potential in the classical molecular dynamics simulation, which includes a long-range force. In this model, we considered an exponentially decreasing electron-density function, a two-body potential function as defined by Rose et al.,[32] and assumed the embedding energy to be a universal form as suggested by Banerjee and Smith.[33] The alloy model of Johnson[34] is applied and an extra parameter is introduced in order to fit dilute-limit heats of solution. The predicted heats of formation for the three possible compounds, namely, $AuPd_3$, AuPd, and Au_3Pd are −0.06, −0.08, and −0.06 eV. The corresponding values from first principle calculations are −0.06, −0.11, and −0.10 eV, respectively. The reasonable agreement between the heats of formation ensures that the Au−Pd alloying potential can be used for a wide range of compositions with good accuracy. Therefore, all the potential forms and parameters in Cai's work are used directly without any modification (see details in ref 31). MD simulations are performed using XMD developed by J. Riffkin.[35] The program employs a predictor−corrector algorithm to integrate the equation of motion and velocity rescaling constant temperature to control system temperature. A time step of 5×10^{-15} seconds (5 fs) is used.

III. Results and Discussion

A. Structural Transformation during Heating. To study the thermal effect on Au−Pd nanocluster, 262-atom decahedral clusters with different Au/Pd compositions and a few structural types are constructed. The gyration diameters of these clusters are about 26 angstrom. These structures include solid solution clusters such as $Au_{131}Pd_{131}$ and $Au_{163}Pd_{99}$, eutecticlike clusters such as $Au_{33}Pd_{229}$, $Au_{229}Pd_{33}$, $Au_{84}Pd_{178}$, and $Au_{178}Pd_{84}$, and core/shell structures such as Pd_{99}-core/Au_{163}-shell and Au_{99}-core/Pd_{163}-shell (see Figure 2). We must mention that the decahedral structures are the most common type of clusters observed in bimetallic Au−Pd colloids.[36] Figure 1 presents structural transformation for the Au-core/Pd-shell, eutecticlike, and solid solution clusters during heating process at a heating rate of 5×10^{11} K/s. Though our heating rate is relatively high and may lead to some overheating causing a shift in transition

* To whom correspondence should be addressed. E-mail: h_b_liu@yahoo.com (H.B.L.); upal@venus.ifuap.buap.mx (U.P.). Fax: +52-222-2295611.

† Instituto Mexicano del Petróleo.

‡ Universidad Autónoma de Puebla.

10.1021/jp056060e CCC: $33.50
Published on Web 02/22/2006

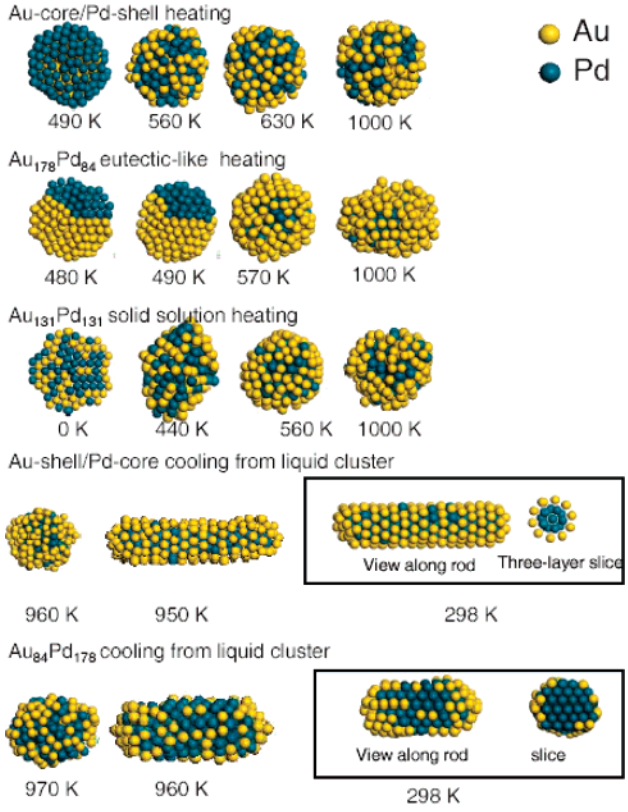

Figure 1. Structural transformations of Au-core/Pd-shell, eutecticlike, and solid-solution clusters during heating and cooling processes.

temperature toward higher values than expected, it should not affect the occurrence of all expected structural transformations. It can be seen from the Figure 1 that the Au-core/Pd-shell clusters retain their structure up to 490 K; change dramatically at 560 K and finally change to Pd-core/Au-shell structure at 630 K. For the eutecticlike $Au_{178}Pd_{84}$ clusters, the structure remains perfect up to 480 K, starts to change at 490 K, and changes to Pd-core/Au-shell structure at 570 K with an incomplete coverage of Au atoms which retains thereafter up to 1000 K. The solid solution $Au_{131}Pd_{131}$ clusters transform to Pd-core/Au-shell structures at about 560 K. In general, Au−Pd bimetallic decahedral clusters with 262 atoms transform to Pd-core/Au-shell clusters at specific temperatures on heating from whatever structures: Au-core/Pd-shell, eutecticlike, solid solution.

To analyze the above-mentioned structural transformation from the point of view of phase transformation, the variation of the total energy per atom with temperature during the heating process is studied for the considered structures. The total energy includes binding energy and kinetic energy. The results are plotted in Figure 2 for all the bimetallic clusters under study. For the sake of clarity, they are plotted in parts a, b, and c of Figure 2 according to their features. In Figure 2a, Pd_{99}-core/Au_{133}-shell and eutecticlike $Au_{229}Pd_{33}$ show the regular features of nonequilibrium melting, with an abrupt slope change between solid and liquid sides. The rest of the clusters take different irregular features. In comparison with the regular nonequilibrium melting (phase transformation), all the irregular melting processes include extra energy decrease. By consideration of the structure transformations shown in Figure 1, it is obvious that the decrease of extra energy is the result of Pd-core/Au-shell formation. Furthermore, the transformation rate from other structures to the Pd-core/Au-shell final structure depends strongly on the initial structure, the transformation path, and the composition of the initial clusters. The Au-core/Pd-shell, eutecticlike $Au_{84}Pd_{178}$ and $Au_{178}Pd_{84}$ clusters shown in Figure 2c, have relatively high structural energy[21] and the Au and Pd atoms are in segregation state, which benefits the collective motion of the atoms, causing the formation of Pd-core/Au-shell structure relatively rapid. On the other hand, the solid-solution

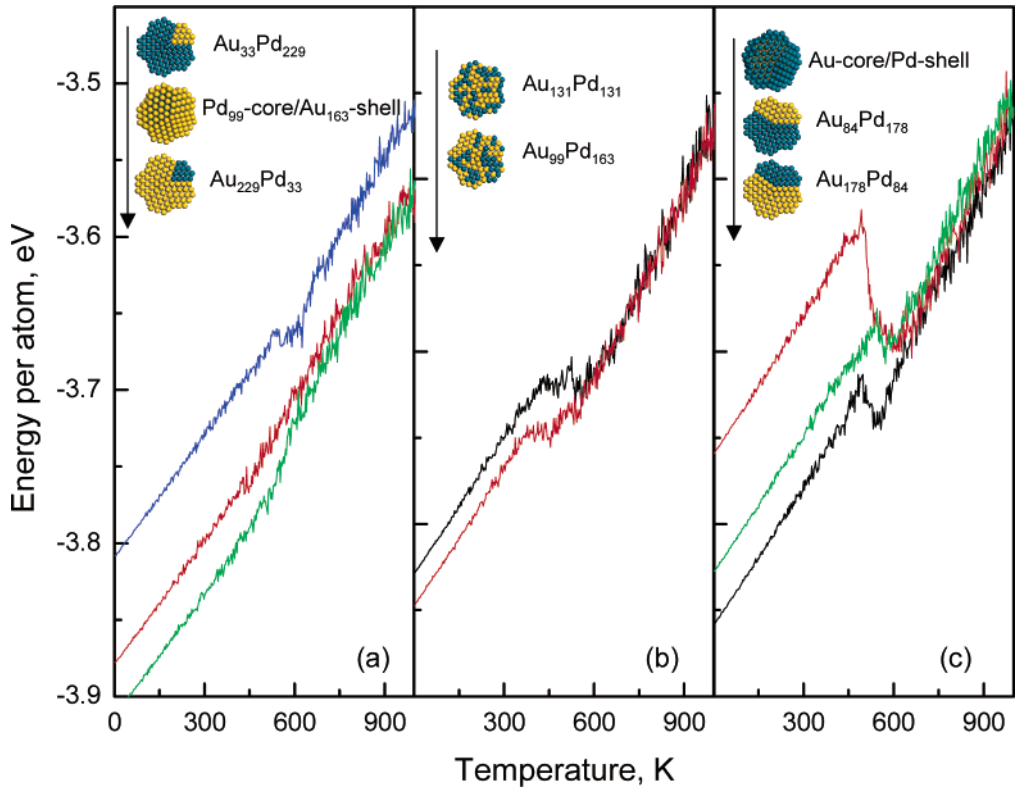

Figure 2. The dependence of energy per atom on temperature during heating process for: (a) $Au_{229}Pd_{33}$ and $Au_{33}Pd_{299}$ and Pd-core/Au-shell, (b) $Au_{131}Pd_{131}$ and $Au_{99}Pd_{163}$, and (c) Au-core/Pd-shell, $Au_{84}Pd_{178}$, and $Au_{178}Pd_{84}$ clusters.

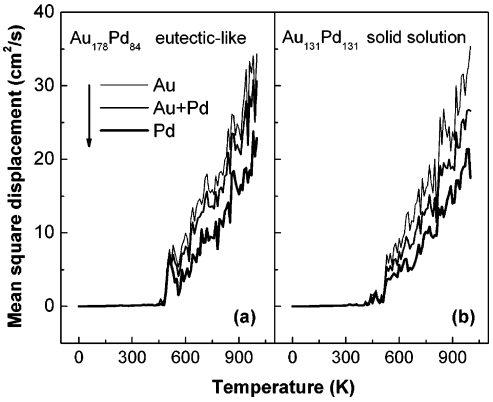

Figure 3. Mean square displacement vs temperatures for the atoms in $Au_{178}Pd_{84}$ eutecticlike and $Au_{131}Pd_{131}$ solid-solution clusters.

clusters transform to Pd-core/Au-shell (Figure 2b) with a relatively slower rate. In the case of eutecticlike $Au_{33}Pd_{229}$ and $Au_{229}Pd_{33}$ clusters (Figure 2a), where the content of one type of atoms is very high and the other is trace, Pd-core/Au-shell transformations display a small amount of energy decrease, even unobservable for $Au_{33}Pd_{229}$ and Pd_{99}-core/Au_{163}-shell clusters.

To clarify the dynamic process in a quantitative way, mean square displacement (MSD) of atoms for all the structures are calculated taking the previous step of the configurations in the trajectory of the heating process as reference (eq 1)

$$\mathrm{MSD} = \langle \mathbf{r}(t) - \mathbf{r}(t - \Delta t)|^2 \rangle \qquad (1)$$

where $\mathbf{r}$ is the position vector of the atom, t is time, Δt is the time step and $\langle\ \rangle$ denotes averaging over all the atoms. In this manner, the MSDs reflect the relative change of diffusivity of atoms at different temperatures more directly. The calculated MSDs for $Au_{178}Pd_{84}$ eutecticlike and $Au_{131}Pd_{131}$ solid-solution clusters are presented in Figure 3. Though the two clusters have different features in the energy curves (Figure 2) near melting, the MSDs of the two are similar, displaying a steep increase of MSD with temperature, indicating that the melting processes occur and finish within a small range of temperature. The Au-core/Pd-shell structures also revealed similar features in their MSD. The melting process is much quicker than the Pd-core/Au-shell formation process. In general, the Pd-core/Au-shell formation process is accompanied by a synchronous and slow melting process. For both $Au_{178}Pd_{84}$ eutecticlike and $Au_{131}Pd_{131}$ solid-solution structures, the resulting Pd-core/Au-shell structure is liquidlike with diffusive motion within the Pd core and Au shell, and relatively little diffusion of Pd atoms into Au shell and vice versa (Figure 3). In addition, for both the structures (eutecticlike and solid solution), MSDs of Au atoms are always larger than those of Pd atoms, which may be attributed to the distribution of Au atoms at the cluster surface.

The formation process of Au-shell/Pd-core structures during heating is further studied by calculating the radial distribution functions (RDF) between unlike-pair atoms. Figure 4a shows the results for $Au_{178}Pd_{84}$ eutecticlike cluster at different temperatures. At 0 K, the RDF is step shaped with minimum value, indicating a regular eutecticlike structure. As the temperature increases up to 570 K, the RDF increases rapidly and thereafter does not change much until 1000 K, indicating a rapid termination of segregation process. For the $Au_{131}Pd_{131}$ solid solution cluster (Figure 4b), the RDF has a maximum value at 0 K. Beyond 440 K, it decreases rapidly until 560 K and then gradually up to 1000 K. The results indicate that the Au-shell/Pd-core formation process in solid solution clusters is slower than that of eutecticlike clusters. It must be noted that, though the temperature of structure transformation for the Au-core/Pd-shell and eutectic clusters are higher than that of the solid solution clusters, the atom segregation process is faster in the latter.

B. Structural Transformation during Cooling. To observe the stability of the structures obtained by the heating process further, cooling processes are performed on them. A very small cooling rate of 5×10^8 K/s was used to obtain fully relaxed structures. It is found that the starting temperature of liquid clusters has a great effect on the cooled structures. We could observe four distinct cases. In the case where the starting temperature is high enough, the cluster may vaporize, as the superheated liquid is fully relaxed. When the starting temperature is relatively high but below the evaporation temperature, the cooled structure may be a three-layer icosahedral nanorod with defects of chemical disorder and deformation. When the starting temperature is just a little higher than melting point, the face-centered cubic (fcc) clusters with {111} surface exposed are preferred. As the starting temperature increases further, the fcc clusters grow more and more fully in the [111] direction and the structures become elongated, even have the shape of a nanorod growing along the [111] direction and faceting most with the {111} surface. As a concrete example, the $Au_{178}Pd_{84}$ cluster revealed all the above-mentioned cooled structures on cooling from different starting temperatures: 1000, 900, 850, and 800 K, respectively. In fact, all the clusters under study were examined and all of them revealed similar characteristic, except that the specific starting temperatures are different for different clusters. Typical icosahedral and fcc nanorods obtained

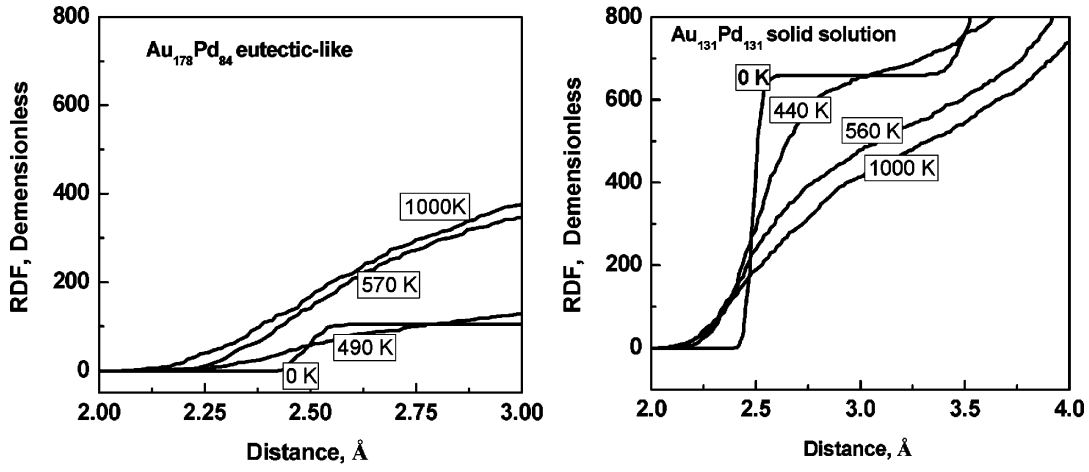

Figure 4. Radial distribution functions of unlike pair for $Au_{178}Pd_{84}$ eutecticlike and $Au_{131}Pd_{131}$ solid-solution clusters.

by cooling the Pd-core/Au-shell and $Au_{84}Pd_{178}$ liquid clusters, respectively, are presented in Figure 1 with two crystallographic views at 298 K. The critical transformation configurations at 960 and 950 K for the former and at 970 and 960 K for the latter are also presented. It has been observed that at 0 K, the icosahedral nanorod is more stable than Pd-core/Au-shell cluster and more stable than solid-solution cluster of similar compositions. For example, at 0 K, the energies per atom for the three structures are −3.86, −3.92, and −3.81, respectively. As a practical stability test at finite temperature, the icosahedral nanorod was heated at a slow rate and seen to be transformed to Pd-core/Au-shell rounded cluster at about 400 K. It must be noted that the Pd-core/Au-shell structure persists in all the cases on heating or further cooling, while a full surface coverage of Au atoms can be obtained only when the Au content is high. When the Au content is low, the Au atoms prefer to occupy the two ends of the nanorods. Additionally, the pure Au and pure Pd clusters were found to acquire similar structures as that of $Au_{178}Pd_{84}$. Therefore, we believe that the initial composition of the clusters does not have a direct effect on the formation of the final structure. However, the composition does affect the melting point, resulting in different starting temperature for generating a particular structure while cooling.

It must be mentioned that the final cooled structure of the clusters depends strongly on the rate of cooling. While a faster cooling rate can lead to the formation of unstable disordered structures, a slower cooling rate leads to the formation of stable well-defined crystalline structures of the clusters. Formation of well-ordered structures with the cooling rate used in our study (5×10^8 K/s) indicates that our cooling rate is adequate for obtaining stable geometrical structures of the clusters.

C. Structural Stability at Finite Temperature. To determine the relative stability of three-layer icosahedral nanorod at finite temperature, Gibbs free energies are calculated for Pd-core/Au-shell decahedron, three-layer icosahedral nanorod and solid-solution decahedron. These three clusters were built with the same number of Au and Pd atoms, so that, the calculated Gibbs free energy can be comparable. The calculation details are as follows.

The velocity autocorrelation function $C(t)$ can be calculated by molecular dynamics simulation[37]

$$C(t) = \langle \mathbf{v}(0) \cdot \mathbf{v}(t) \rangle \tag{2}$$

where $\mathbf{v}(t)$ is atom velocity at time t and $\langle\ \rangle$ denotes the ensemble average. The Fourier transform of velocity autocorrelation function is the phonon density of states $S(\upsilon)$, given by

$$S(\nu) = \frac{2}{k_B T}\int_{-\infty}^{\infty} C(t) e^{-i2\pi\nu t}\, dt \tag{3}$$

where k_B is Boltzmann's constant. The density of states $S(\upsilon)$ satisfies $\int_{0\infty} S(\nu) d\nu = 3N$, where N is the number of atom and $3N$ is the total number of phonon modes. Under the harmonic approximation, the partition function can be expressed as

$$\ln Q = \int_0^{\infty} d\nu S(\nu) \ln \frac{\exp(-\beta h\nu/2)}{1 - \exp(-\beta h\nu/2)} \tag{4}$$

where $\beta = 1/k_B T$, h is Planck constant. The vibrational entropy is determined by the partition function

$$S_{vib} = k_B \ln Q + \beta^{-1}\left(\frac{\partial \ln Q}{\partial T}\right)_{N,V} \tag{5}$$

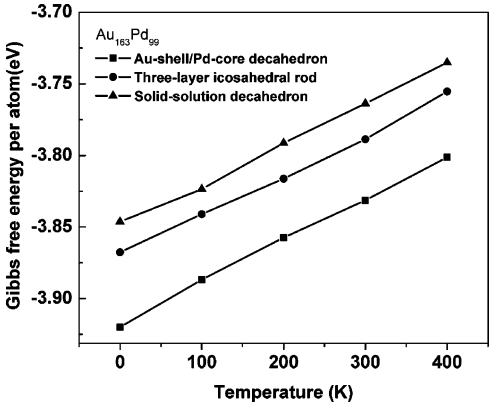

Figure 5. Temperature dependence of Gibbs free energy for Pd-core/Au-shell, solid solution, and three-layer icosahedral nanorod with 163 Au and 99 Pd atoms.

On the other hand, the configurational entropy can be calculated using the equation

$$S_{con} = k_B \ln w \tag{6}$$

where w is the number of possible configurations. For random solid solution, the configurational entropy reaches the maximum of 0.014991 eV/K. For Au-shell/Pd-core structure and the perfect three-layer icosahedral nanorod, the number of possible configuration is one. At very low temperatures, there exist only a small amount of chemical disorders and structural defects, and the configurational entropy can be roughly estimated by the observed defect concentration. Finally, the Gibbs free energy is determined by the calculated entropy and total energy E_{tot} from molecular dynamics simulation using the relation

$$G = E_{tot} - T(S_{vib} + S_{con}) \tag{7}$$

The total energy E_{tot} calculation was converged to 1×10^{-7} eV in order to enhance the degree of accuracy in calculated Gibbs free energy. The resulting Gibbs free energies are displayed in Figure 5. It is obvious that the three-layer icosahedral nanorod is not as stable as the Pd-core/Au-shell decahedron; however it is more stable than solid-solution decahedron. Experimentally it is observed that various structures such as Pd-core/Au-shell, Au-core/Pd-shell, and solid-solution-like can be synthesized, and depending on the synthesis conditions their shapes can be retained up to a certain range of temperature.[27] That is to say, when the three-layer icosahedral rod is formed by cooling process, it is stable for a certain range of temperature. In our study, it is found that the three-layer icosahedral rod keeps its structure up to 400 K and then transforms rapidly to rounded structure before reaching 425 K.

IV. Conclusions

In summary, Pd-core/Au-shell structures can be formed by annealing whatever structure: Au-core/Pd-shell, eutecticlike, or solid solution. The Pd-core/Au-shell structure persists for all the cases on cooling from the temperatures beyond their corresponding melting points. Depending on the starting temperature, the heated structures can be cooled to three-layer icosahedral nanorod, fcc nanorod, or fcc clusters. The three-layer metastable icosahedral nanorod is not as stable as the Au-shell/Pd-core decahedron. However, it is more stable than the solid-solution decahedron and can retain its structure up to about 400 K. This metastable rod structure can be used in catalysis at room temperature or at temperatures below 400 K. Though the

composition of the bimetallic clusters does not have a direct effect on the geometry of the final structures while heating or cooling, it does affect their melting points, which define the temperatures from where they should be cooled to obtain a particular structure. Our results on the phase and structure transformation have important implications in heterogeneous catalysis especially while using such bimetallic clusters at high temperatures, and for the synthesis of their selective structures. While for high-temperature catalytic use, one should take care of calcination temperature to retain the original cluster structure, by manipulating the temperature of synthesis or annealing temperature, one can obtain the nanostructures of selective shape.

Acknowledgment. U. Pal acknowledges partial financial supports from VIEP (BUAP)-SEP and CONACyT, Mexico, through Grant Nos. 11//EXC/05 and 46269, respectively.

References and Notes

(1) Jellinek, J.; Krissinel, E. B. *Theory of Atomic and Molecular Clusters*; Springer: Berlin, 1999.

(2) Shibata, T.; Bunker, B. A.; Zhang, Z.; Meisel, D.; Vardeman, C. F.; Gezelter, J. D. *J. Am. Chem.* Soc. **2002**, *124*, 11989.

(3) Molenbroek, A. M.; Haukka, S.; Clausen, B. S. *J. Phys. Chem. B* **1998**, *102*, 10680.

(4) Darby, S.; Thomas, V.; Johnston, R. L.; Roberts C. J. *Chem. Phys.* **2002**, *116*, 1536.

(5) Kreibig, U.; Vollmer, M. *Optical Properties of Metal Clusters*; Springer: Berlin, 1995.

(6) Rossi, G.; Rapallo, A.; Mottet, C.; Fortunelli, A.; Baletto, F.; Ferrando, R. *Phys. Rev. Lett.* **2004**, *93*, 105503.

(7) Gaudry, M.; Cottancin, E.; Pellarin, M.; Lermé, J.; Arnaud, L.; Huntzinger, J. R.; Vialle, J. L.; Broyer, M. *Phys. Rev. B* **2004**, *67*, 155409.

(8) Hu, J. W.; Zhang, Y.; Y. Li, Y.; Liu, Z.; Ren, B.; Sun, S. G.; Tian, Z. Q.; Lian, T. *Chem. Phys. Lett.* **2005**, *408*, 354.

(9) Mainardi, D. S.; Balbuena, P. B. *Int. J. Quantum Chem.* **2001**, *85*, 580.

(10) Venezia, A. M.; La Parola, V.; Nicoli, V.; Deganello, G. *J. Catal.* **2002**, *212*, 56.

(11) Landon, P.; Collier, P. J.; Carley, A. F.; Chadwick, D.; Papworth, A. J.; Burrows, A.; Kiely, C. J.; Hutchings, G. *J. Phys. Chem. Chem. Phys.* **2003**, *5*, 1917.

(12) Benedetti, A.; Bertoldo, L.; Canton, P.; Goerigk, G.; Pinna, F.; Riello, P.; Polizzi, S. *Catal. Today* **1999**, *49*, 485.

(13) Lemire, C.; Meyer, R.; Shaikhutdinov, S.; Freund, H. J. *Angew. Chem., Int. Edit.* **2004**, *43*, 118.

(14) Enomoto, A.; Kurokawa, S.; Sakai, A. *Phys. Rev. B* **2002**, *65*, 125410.

(15) Tran, N. T.; Powell, D. R.; Dahl, L. F. *J. Chem. Soc., Dalton Trans.* **2004**, *2*, 217.

(16) Venezia, A. M.; La Parola, V.; Deganello, G.; Pawelec, B.; Fierro, J. L. G. *J. Catal.* **2003**, *215*, 317.

(17) Pawelec, B.; Venezia, A. M.; La Parola, V.; Cano-Serrano, E.; Campos-Martin, J. M.; Fierro, J. L. G. *Appl. Surf. Sci.* **2005**, *242*, 380.

(18) Chen, Y. H.; Tseng, Y. H.; Yeh, C. C. *J. Mater. Chem.* **2002**, *12*, 1419.

(19) Cardenas, G.; Segura, R. *Mater. Res. Bull.* **2000**, *35*, 1369.

(20) Oshima, R.; Yamamoto, T. A.; Mizukoshi, Y.; Nagata, Y.; Maeda, Y. *Nano. Mater.* **1999**, *12*, Part A Sp. Iss. SI, 111.

(21) Robach, Y.; Abel, M.; Porte, L. *Surf. Sci.* **2003**, *526*, 248.

(22) Gimenez, M. C.; Leiva, E. P. M. *Langmuir* **2003**, *19*, 10538.

(23) Chang, H. S.; Hsieh, K. C.; Martens, T.; Yang, A. J. *Electron Mater.* **2003**, *32*, 1182.

(24) Lehmann, F.; Richter, G.; Borzenko, T.; Hock, V.; Schmidt, G.; Molenkamp, L. W. *Microelectron. Eng.* **2003**, *65*, 327.

(25) Kan, C. X.; Cai, W. P.; Li, C. C.; Zhang, L. D.; Hofmeister, H. *J. Phys. D* **2003**, *36*, 1609.

(26) Wu, M. L.; Chen, D. H.; Huang, T. C. *Langmuir* **2001**, *17*, 3877.

(27) Toshima, N. *Pure Appl. Chem.* **2000**, *72*, 317.

(28) http://cyberbuzz.gatech.edu/asm_tms/phase_diagrams/pd/au_pd-.jpg.

(29) Hultgren, R.; Desai, P. D.; Hawkins, D. T.; Gleiser, M.; Kelley, K. K. *Selected Values of thermodynamic Properties of Binary Alloys*; American Society for Metals Park: Metal Park, OH, 1973.

(30) Liu, H. B.; Pal, U.; Medina, A.; Maldonado, C.; Ascencio, J. A. *Phys. Rev. B* **2005**, *71*, 075403.

(31) Cai, J.; Ye, Y. Y. *Phys. Rev. B* **1996**, *54*, 8398.

(32) Banerjee A.; Smith, J. R. *Phys. Rev. B* **1988**, *37*, 6632.

(33) Johnson, R. A. *Phys. Rev. B* **1989**, *39*, 12554.

(34) Rose, J. H.; Smith, J. R.; Guinea, F.; Ferrante, J. *Phys. Rev. B* **1984**, *29*, 2963.

(35) Riffkin, J. Center of Simulation, University of Connecticut, 2004, http://www.ims.uconn.edu/centers/simul.

(36) Rodriguez-Lopez, J. L.; Motejano-carrizales, J. M.; Pal, U.; Sanchez-Ramirez, J. F.; Troiani, H.; Garcia, D.; Miki-Yoshida, M.; Jose-Yacaman, M. *Phys. Rev. Lett.* **2004**, *92*, 196102.

(37) Frenkel, D.; Smit, B. *Understanding Molecular Simulation from Algorithms to Applications*; Academic Press: New York, 2002.